

## THE SMOOTHNESS OF CO LINE PROFILES IN ORION: IMPLICATIONS FOR CLUMPINESS

JAN A. TAUBER,<sup>1,2</sup> PAUL F. GOLDSMITH,<sup>2</sup> AND ROBERT L. DICKMAN<sup>2</sup>*Received 1990 August 1; accepted 1991 January 9*

## ABSTRACT

We have obtained spectra with very high signal-to-noise ratio and spectral resolution of the  $^{12}\text{CO}$  and  $^{13}\text{CO } J = 1 \rightarrow 0$  transitions toward several positions in the Orion region. These observations test the extent to which the clumpy structure of this region is reflected in the velocity structure of the spectra. The smoothness of the profiles is such that if the cloud is assumed to have a constant clump volume filling factor, an unrealistically large number of clumps is necessary to reproduce the observations. A volume filling factor which increases from a small value at the surface to a large value at the core may be more appropriate for this source.

*Subject headings:* interstellar: molecules — line profiles — nebulae: internal motions

## 1. INTRODUCTION

In recent years it has become clear that Giant Molecular Clouds (GMCs) are clumpy, i.e., they exhibit large point to point density fluctuations. This has been observed on large spatial scales (e.g., Bally et al. 1987) and with the advent of millimeter-wave interferometry also on very small spatial scales (e.g., Wilson & Johnston 1989; Mundy et al. 1989). The existence of clumpiness has recently been linked to the long-recognized problem of reconciling the large widths of molecular line emission from GMCs with expected cloud lifetimes and energy dissipation rates. Earlier explanations for the line-widths involving systematic velocity fields and/or microturbulent motions have fundamental flaws (see Baker 1976 for a brief review). In an attempt to resolve these difficulties, Kwan & Sanders (1986) developed a model in which molecular clouds are formed from smaller gas units (clumps) which have purely thermal internal motions, but whose motions within the cloud are suprathermal. Thus, the wide lines observed with an antenna beam which does not resolve the clumps are a superposition of the narrower lines emitted by individual clumps. If this is the case, the shape of the observed line profiles should reflect some of the properties of the underlying clumps, such as their intrinsic line width, the distribution of their velocities within the cloud, and possibly even their number. Unfortunately, in most studies of line emission from GMCs, very little attention is paid to the details of the line profiles observed. In part this is a consequence of the perception that most lines appear to be featureless, usually approximating smooth Gaussians to a large degree. However, the nagging question remains: is the lack of features in the profiles due to inadequate signal-to-noise ratio and/or velocity resolution?

Stutzki & Güsten (1990) have observed a number of CO and CS transitions in the M17 GMC. Their results show that there is a significant increase in the velocity structure of the observed profiles as the angular resolution increases. Via a complicated deconvolution algorithm, they derive a distribution of the line widths of clumps in this region. The distribution peaks at  $\sim 1 \text{ km s}^{-1}$  (well above the expected thermal width), but some

clumps have line widths as low as  $\sim 0.5 \text{ km s}^{-1}$ . Although a significant fraction of the clumps are spatially unresolved, the work of Stutzki and Güsten shows unambiguously that at least in some GMCs there is gas clumping on small size scales ( $\sim 0.1 \text{ pc}$ ), and that individual clump line widths are narrower than the velocity extent of their parent cloud.

It is unclear what angular resolution is necessary to obtain a complete picture of the mass and line width distribution of the constituent clumps of a typical molecular cloud. At high angular resolution, interferometry has in several instances resolved clumps in GMCs. The technique, however, only yields information on a small region of the GMC, information which is usually limited to a subset of the full range of spatial Fourier components. On the other hand, observations of GMCs at moderate angular resolution should yield information on relatively large regions of the clouds, and thus have the potential to trace clump characteristics through the GMCs.

In this paper, we approach the issue of clump velocities by analyzing molecular line profiles having very high signal-to-noise ratio, and a velocity resolution adequate to resolve thermal motions. The smoothness of the emission profiles provides indirect information on the otherwise unresolved density and velocity structure within the antenna beam which serves to constrain theoretical cloud models based on the existence of a distribution of dense clumps (e.g., Kwan & Sanders 1986). Our choice of source—Orion—and molecular lines—CO and  $^{13}\text{CO}$ —is directed toward this last goal.

In the next two sections of this paper we discuss the observations and their analysis. In the last section we develop a simplified model which permits us to derive some conclusions about the physical properties of the Orion cloud.

## 2. OBSERVATIONS

Since obtaining data of the quality required for the analysis that we attempt here requires a large experimental effort (both in integration time and in minimizing adverse instrumental effects), we have concentrated our observations on only a few selected points of a single molecular cloud, Orion A. This is the closest GMC with ongoing massive star formation activity (see Genzel & Stutzki 1989 for an extensive review of observations of this region). We have observed positions that cover a range of line intensity and optical depth, concentrating on four positions in a north-south strip starting at the position of the Kleinmann-Low object (KL), and stepping north in 3' steps.

<sup>1</sup> Radio Astronomy Laboratory, 601 Campbell Hall, University of California, Berkeley, CA 94720 (postal address for J. A. T.).

<sup>2</sup> FCRAO, Department of Physics and Astronomy, 626 Lederle Research Tower B, University of Massachusetts, Amherst, MA 01003 (postal address for P. F. G. and R. L. D.).

Both the  $^{12}\text{CO}$  and  $^{13}\text{CO}$   $J = 1 \rightarrow 0$  transitions were observed at each position, except for the position 3' north of KL, for which the  $^{13}\text{CO}$  observation was displaced by 0.5 north. At the most northerly of the observed positions (9' from KL), the gas column density obtained from a standard calculation which uses the lower three rotational transitions of CO and  $^{13}\text{CO}$  has decreased by a factor of  $\sim 10$  from its value at KL (Tauber 1990).

The observations were conducted in 1988 and 1989 with the 14 m telescope of the Five College Radio Astronomy Observatory, using a cooled Schottky-diode heterodyne receiver. Only data taken during stable weather conditions were used. The data were calibrated using the chopper-wheel technique of Penzias & Burrus (1973), and no second-order corrections to account for atmospheric effects were made. All the data shown in this paper are given in units of  $T_A^*$ , as defined in Kutner & Ulich (1981). The angular resolution of the 14 m telescope is  $\sim 45''$ , which at the distance of Orion ( $\sim 500$  pc) corresponds to a linear resolution of  $\sim 0.11$  pc. This is somewhat higher than the 0.14 pc linear resolution obtained by Stutzki & Güsten (1990) in M17.

The backend used was a 256 channel spectrometer with 100 kHz resolution per filter element. This filterbank was preceded by a spectrum expander (Henry 1979) set to an expansion factor of 4, so that the nominal resolution of each channel was 25 kHz. Since the expander is inherently nonlinear, an average chopper-wheel calibration was determined from a parallel  $256 \times 1$  MHz filterbank and applied to all the high-resolution channels. At 115 GHz, the velocity resolution afforded by a 25 kHz filter is  $0.065 \text{ km s}^{-1}$ , adequate to resolve the thermal motions of CO above a kinetic temperature of 10 K.

Any spectrometer may distort an observed line profile. The most straightforward effects are due to nonlinearity of the channel detectors (presumably similar for all channels), and to channel-to-channel differences in the detector linearity coefficients (power to voltage conversion). The first effect acts to reduce or enhance the contrast in the profile structure by compressing or stretching the temperature scale. We tested for this effect by integrating on an ambient temperature load and switching different levels of attenuation into the signal. This permits the easy identification and subsequent elimination of grossly nonlinear channels. The test showed that all channels have a slightly nonlinear behavior, resulting in a stretch of the  $T_A^*$  scale by  $\sim 2\%$  for values of  $T_A^*$  near 50 K.

The dispersion of this nonlinearity across the channels (the second effect mentioned above) was found to be potentially important for integrations exceeding several hours. However, on such time scales the effect cannot be studied easily owing to the lack of a noise source whose power output is stable over a long period. In order to avoid distortions of our data arising from this effect, we successively shifted the center frequency of the filterbank by a few channels, typically after every 2 minutes of integration. Since the final result is obtained by averaging individual integrations, the total usable width of the filterbank is reduced by the same amount that its center frequency has been changed. This technique "homogenizes" the conversion of power to voltage across the filterbank by averaging the individual deviations from linearity over a large number of detectors and can be thought of as "sliding" the observed line across the filterbank. Because the nonlinearity of an individual channel in the final spectrum is the average nonlinearity of the detectors involved, the resulting dispersion of the nonlinearity is reduced by a factor equal to the square root of the number of

detectors involved (assuming that the coefficients of nonlinear terms are normally distributed about some mean value). An additional benefit of this technique is that any standing waves in the receiver system are effectively averaged out by scrambling their phases in velocity space.

Another important consideration relating to the backend is the extent to which contiguous channels are correlated. In general, the filter channels of any spectrometer overlap to some degree, and a digital spectrum expander might be expected to introduce additional correlation between adjacent channels. One can test for the significance of channel overlap by plotting channel-to-channel correlation diagrams (Bracewell 1978). In Figure 1 we show typical correlation diagrams for the receiver/backend configuration that we have used. Figure 1a was generated by plotting the power levels measured on Jupiter in every channel, versus the power level measured in the corresponding adjacent channels. A clear correlation can be seen in this diagram. Figure 1b is similar, but on the vertical axis we have plotted the power in the next-to-adjacent channel. This figure is essentially a scatter diagram. Thus, the effective bandwidth of each channel in our experiment lies somewhere between 25 and 50 kHz, with the exact filter bandwidth unknown. This test underlines the importance of having an adequate segment of emissionless baseline in the observed spectrum since this is the only certain means by which to evaluate the noise in the profile.

Since we want to avoid artificial correlations in our profiles, we have opted to discard every second channel in the observed spectra. From here on we therefore assume that the frequency resolution of the spectra is 50 kHz per channel, corresponding to a velocity resolution of  $0.13 \text{ km s}^{-1}$  at 115 GHz.

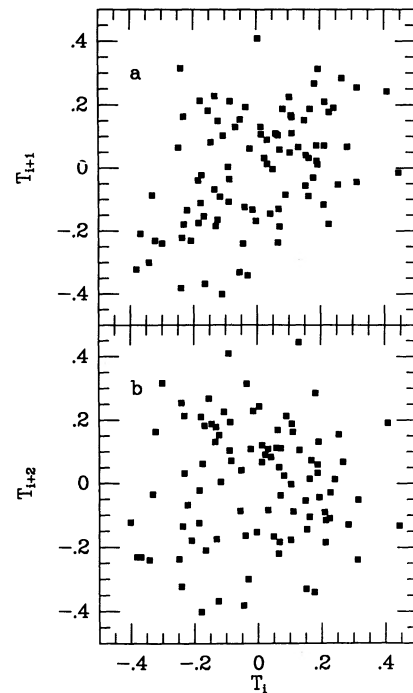


FIG. 1.—Correlation diagrams of the noise in the receiver/backend system, obtained after integration on the planet Jupiter. A constant DC offset has been subtracted from all channels. (a) The temperature in each channel is plotted vs. the temperature in the adjacent channel. The correlation coefficient is  $\sim 0.4$ . (b) The temperature in each channel is measured vs. the temperature in the next-to-adjacent channel. The correlation coefficient is  $\sim 0.1$ .

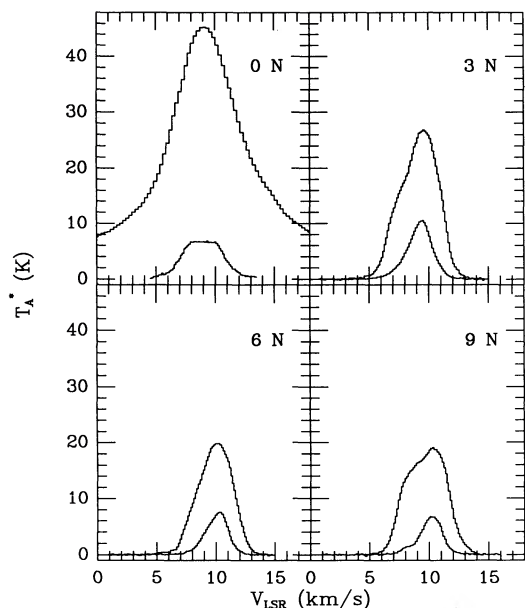


FIG. 2.—The observed antenna temperature vs. LSR velocity profiles of  $^{12}\text{CO } J=1 \rightarrow 0$  and  $^{13}\text{CO } J=1 \rightarrow 0$  are shown to the same scale. The observed positions are as indicated in the figure, except for  $^{13}\text{CO } J=1 \rightarrow 0$  at 3 N, which was actually observed at 3.5 N. The central position is located near the Kleinmann-Low object, at R.A.  $05^{\text{h}}32^{\text{m}}47^{\text{s}}$  and  $\delta = 05^{\circ}24'00''$ .

We present the observed average spectra in Figure 2. The positions at which the spectra were taken are denoted by their offsets from KL in arcminutes, and their basic characteristics are given in Table 1. Qualitative differences in the spectra at different positions are immediately apparent. While we leave aside discussion of the CO spectrum observed toward KL, because of the confusion created by the high-velocity source, we draw attention to the extremely interesting, flat-topped appearance of the  $^{13}\text{CO}$  profile toward this position.

North of KL, all the spectra show an extraordinarily smooth appearance on the scale of a few channels (a few small features are noticeable on the  $^{12}\text{CO}$  profile at 9 N). One does see, however, some structure on velocity scales of the order of the widths of the lines themselves. Indeed, at 3 N and 9 N one can clearly distinguish at least two velocity components, most noticeably in the  $^{12}\text{CO}$  lines. These components probably arise in regions of different physical characteristics, since the  $^{12}\text{CO}$  to  $^{13}\text{CO}$  ratios for each component are quite different. Thus, a direct visual inspection of the spectra suggests the existence of dynamical or chemical coherence at large scales (large in mass and size), but not at small scales.

We note that even though our observations have better

TABLE 1  
GENERAL CHARACTERISTICS OF THE OBSERVED PROFILES

Line	Position	$T_A^*$ (peak) (K)	Width ( $\text{km s}^{-1}$ )	Baseline rms (K) <sup>a</sup>	S/N <sup>b</sup>
$^{12}\text{CO}$ .....	3 N	27.0	3.9	0.09	280
$^{13}\text{CO}$ .....	3.5 N	10.3	2.8	0.05	230
$^{12}\text{CO}$ .....	6 N	20.0	3.6	0.07	285
$^{13}\text{CO}$ .....	6 N	7.3	2.5	0.05	150
$^{12}\text{CO}$ .....	9 N	19.0	3.9	0.05	358
$^{13}\text{CO}$ .....	9 N	6.6	2.6	0.07	100

<sup>a</sup> In 50 kHz wide channel.

<sup>b</sup> Peak  $T_A^*$  divided by baseline rms noise.

linear resolution and signal-to-noise ratios than those of Stutzki & Güsten (1990) in M17, they show much less velocity structure. Both regions have similar physical characteristics, and are both illuminated by intense UV sources; the main difference between them seems to lie in their geometrical orientation with respect to the observer. In effect, the ionizing stars in Orion are in the line of sight between the observer and the cloud, whereas in M17 they are situated away from the cloud in the plane of the sky. The consequence of this is that lines of sight directed toward KL traverse the core of the Orion cloud, whereas lines of sight directed toward the bright rim in M17 only probe the edge of the cloud. Thus, the lack of velocity structure in the line profiles from Orion relative to those from M17 may be due to the fact that in Orion the spectra carry information on a large portion of the cloud. This idea is reasonable if both clouds are clumpy, in which case the number and the characteristics of the clumps probed in each cloud are potentially very different.

### 3. ANALYSIS OF THE PROFILES

The analysis of the velocity structure of an observed spectral line profile should ideally yield a number (or set of numbers) which would permit a comparison of the line smoothness for different velocity ranges within a given profile (e.g., line core vs. wings), from spectrum to spectrum within a single cloud, and even from cloud to cloud. We have found (Tauber 1990) that this is possible only if one is willing to make a *comparative* analysis of the smoothness relative to some arbitrary standard, a good choice of which is a Gaussian. However, this procedure is physically unattractive in the context of a clumpy cloud model because it presupposes that the line-of-sight velocities of the clumps are normally distributed and thus only allows us to measure statistical deviations from this ideal behavior. We have explored this type of analysis in considerable detail (Tauber 1990) but find it to be of limited use for the observations discussed in this paper, due to the extreme smoothness of the spectra.

The Fourier power spectrum is an alternative analytical tool which can be implemented with the help of standard numerical techniques. We have found this to be the most useful technique for studying the extremely smooth profiles that we have observed in Orion.

In Figure 3 we plot the power spectra (PS) of the profiles as a function of wavenumber. The PS cover the wavenumber ( $\lambda$ ) range between 0 and the Nyquist wavenumber, equal to that determined by the velocity sampling interval  $\delta v$ ,  $\lambda_{\text{Ny}} = 1/(2\delta v)$ . For the present data  $\delta v = 0.13 \text{ km s}^{-1}$ . In this and subsequent plots, wavenumber has been normalized by twice the Nyquist wavenumber; hence, the maximum normalized wavenumber is 0.5. Hereafter, when we say wavenumber, it should be taken to mean normalized wavenumber. We define an equivalent Gaussian for each observed profile as a Gaussian with FWHM equal to  $(2)^{1/2}\omega$ , where  $\omega$  is the width of the autocorrelation function (ACF; see Bracewell 1978 for definitions and discussion) of the observed profile. We use the width of the ACF rather than the width of the profile because the former does not depend on the choice of a center velocity. The power spectra of the equivalent Gaussian profiles are shown in Figure 4, where we have added randomly generated Gaussian noise to produce the same signal-to-noise level as in the astronomical spectra. It is clear that all the observed profiles show power in excess of their Gaussian equivalents. Much of this power may simply arise from the large-scale asymmetries of the profiles.

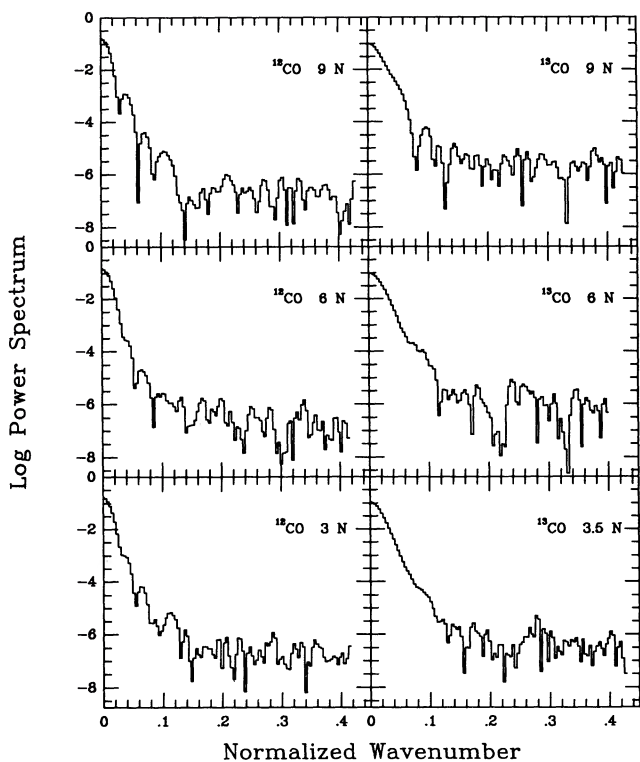


FIG. 3.—The logarithm of the periodogram estimates of the power spectra of the observed profiles are plotted vs. wavenumber. The power spectra are normalized so that the total power in the observed profile is unity. Wavenumbers are normalized by twice the Nyquist wavenumber (see text for details).

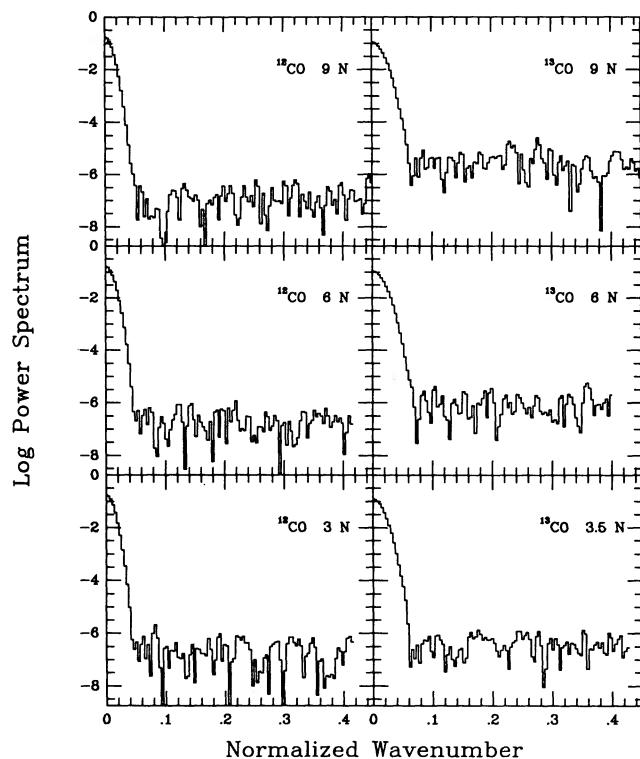


FIG. 4.—Same as in Fig. 3, but these plots correspond to the equivalent Gaussians (as defined in text) of the observed profiles.

An inspection of the observed profiles and their PS yields the following:

1. There are no features in the PS of the observed profiles which would correspond to well-defined “correlation lengths” in velocity space for wavenumbers above  $\sim 0.15$  (Fig. 3). This indicates that the observed  $^{12}\text{CO}$  and  $^{13}\text{CO}$  profiles are smooth down to the noise level for velocity correlation lengths of roughly seven channels or less (corresponding to  $\approx 0.9 \text{ km s}^{-1}$ ).<sup>3</sup> However, the PS show some evidence of structure near the noise level at velocity correlation lengths of  $\sim 1.2 \text{ km s}^{-1}$  (most noticeably for  $^{12}\text{CO}$ ). This is confirmed by the presence of a few individual intensity features in every profile. These were identified by fitting polynomials to small segments of the total velocity extent of each profile, and comparing the rms residuals to the rms noise in the baseline. Typical intensities and widths for features on the  $^{12}\text{CO}$  lines are  $\Delta T \approx 0.4 \text{ K}$ ,  $\Delta v \approx 0.7 \text{ km s}^{-1}$ ; those on the  $^{13}\text{CO}$  lines have  $\Delta T \approx 0.2 \text{ K}$  and  $\Delta v \approx 0.5 \text{ km s}^{-1}$ .

2. At longer velocity correlation lengths ( $> 2 \text{ km s}^{-1}$ ), there is evidence for some structure, with a typical intensity contrast of a few times the rms of the baseline. This type of structure can be directly discerned in velocity space, especially at the 3 N and 9 N positions.

3. The large-scale velocity space shapes of the  $^{12}\text{CO}$  profiles are in general better represented by Gaussians than are those of  $^{13}\text{CO}$  (Figs. 3 and 4). As a consequence, the relative spectral power contribution at high wavenumbers is smaller for  $^{12}\text{CO}$  than for the rare isotope, whose profiles appear relatively more centrally peaked. However, deviations of the PS from Gaussian behavior occur at roughly the same wavenumber for all profiles. Similarly, all profiles show power in excess of the equivalent Gaussian out to about the same wavenumber.

4. There seems to be no obvious correlation between distance from the core of the cloud and line profile smoothness, in spite of the large variation in column density among the observed positions.

5. There is no appreciable difference in the amount of velocity structure found in the wings from that found in the cores of the lines.

#### 4. DISCUSSION

Two idealized models of a clumpy molecular cloud can be readily formulated. In the first, the clumps have a constant volume filling factor throughout the cloud and the observed line intensity at each velocity consists of the combined contribution of many clumps, each weighted by an area covering factor. In the second model, the volume filling factor of clumps varies in some systematic fashion through the cloud. A reasonable way in which this may happen in a cloud in which gravity plays a major role is if the filling factor increases from the surface toward the core of the cloud. This type of structure is suggested by multitransition studies of CS emission from other regions with characteristics similar to those of the Orion cloud (Snell et al. 1984). In this paper we discuss the implications of the first model (constant volume filling factor) and we argue, based on the observations that we have described, that it is unrealistically simple, and that the more complex model of Kwan & Sanders (1986) should be pursued in order to interpret the observations. This has been carried out as described

<sup>3</sup> Note that a  $\delta$ -function in wavenumber space at a normalized wavenumber  $\lambda_0$  corresponds to a velocity “correlation length” of  $\Delta v = \delta v / \lambda_0$ .

briefly in Tauber & Goldsmith (1990), and shall be presented in more detail in a forthcoming publication.

Our model cloud consists of a total number  $N$  of identical clumps which are distributed in (line of sight) velocity with a probability distribution  $P(v)$ . Then the expectation value for the number of clumps with velocities between  $v$  and  $v + dv$  is

$$\langle N_v dv \rangle = NP(v)dv . \quad (1)$$

$P(v)$  must be normalized so that its integral over the full velocity range of the distribution is unity. In the following discussion of the properties of the model we shall omit for clarity the rigorous statistical notation required by its nature (e.g., expectation value brackets). However, the context should make it obvious where this notation is required.

If the clumps are optically thick, and if they do not shadow each other in phase space (by this we mean that no two clumps are simultaneously in the same line of sight and emitting in the same range of velocities), then the emission measured at a certain velocity by an antenna whose beam includes the structure is the combined emission of all clumps at that line-of-sight velocity, weighted by an area filling factor  $f_0$ . If each clump emits a Gaussian line with a characteristic width  $\Delta v_c$ , then the measured antenna temperature can be written as

$$T(v) = T_0 f_v , \quad (2)$$

where

$$\begin{aligned} f_v &= \frac{1}{\delta v} \int_{\delta v} \int_{-\infty}^{\infty} \frac{A_c}{B} N_{v'} \exp \left[ - \left( \frac{v' - v}{\Delta v_c} \right)^2 \right] dv' dv \\ &= \frac{f_0}{\delta v} \int_{\delta v} \int_{-\infty}^{\infty} N_{v'} \exp \left[ - \left( \frac{v' - v}{\Delta v_c} \right)^2 \right] dv' dv . \end{aligned} \quad (3)$$

$T_0$  is the peak antenna temperature which would be emitted by a single clump which fills the antenna beam,  $A_c$  is the area of a single clump,  $B$  the projected area of the beam, and the first integration is over the observed velocity interval (i.e., the width  $\delta v$  of the spectral channel). If the clump line-of-sight velocities are normally distributed about  $v = 0$ , we can write

$$P(v)dv = \frac{1}{\sqrt{\pi} \Delta v} \exp \left[ - \left( \frac{v}{\Delta v} \right)^2 \right] dv , \quad (4)$$

where  $\Delta v$  defines the dispersion of clump velocities within the beam. This parameter is roughly equal to the width of the observed spectral line if the line width of a single clump is much smaller than the dispersion of the ensemble.

As we go toward the wings of the line (with  $\delta v$  constant),  $\int N_v dv$  will decrease and the fractional fluctuations will increase since we sample a smaller number of clumps. However, for a given integration time, the signal-to-noise ratio drops in proportion to the antenna temperature at a particular velocity and hence as the *square* of the relative fluctuations, so that in practice, it will usually be more difficult to measure fluctuations near the edge of the line than at the line center. If we keep near the center of the line ( $v \simeq 0$ ,  $\delta v \ll \Delta v$ ), and if we assume that the width of lines emitted by clumps is small compared to the total line width ( $\Delta v_c \ll \Delta v$ ), we can approximate

$$\begin{aligned} \int_{\delta v} \int_{-\infty}^{\infty} N_{v'} \exp \left[ - \left( \frac{v' - v}{\Delta v_c} \right)^2 \right] dv' dv &\simeq N \\ &\times \int_{\delta v} P(v \simeq 0) \frac{\Delta v_c}{\Delta v} dv \simeq \frac{N \Delta v_c}{\Delta v} \delta v . \end{aligned} \quad (5)$$

In this simple model, we expect the fluctuations in the measured antenna temperature to be caused by the presence or absence of clumps; thus, we can draw their statistics from a Poisson distribution,

$$\Delta T(v) = T_0 \Delta f_v \simeq T_0 f_0 \sqrt{N \Delta v_c / \Delta v} . \quad (6)$$

The fractional fluctuations in the observed antenna temperature will then be

$$\frac{\Delta T(v)}{T(v)} \simeq \frac{1}{\sqrt{N \Delta v_c / \Delta v}} . \quad (7)$$

This expression reflects the intuitively reasonable result that, for a given number of clumps, a wider clump profile results in a smoother overall line shape. The fluctuations of equation (7) will be present on velocity scales ("correlation lengths") on the order of the emission line width of individual clumps. The lower limit for this width is given by their thermal dispersion,  $\Delta v_{th}$ . An upper limit, which would avoid the presence of strong internal shocks within the clumps, is set by the adiabatic soundspeed. We can choose the width of the spectrometer channel to be  $\delta v \simeq \Delta v_c \simeq \Delta v_{th}$ . If we do not recognize any fluctuations in an observed profile down to a given noise level  $T_{rms}$ , we can set a limit on the number of clumps in the beam using the expression for the fluctuations expected in an interval  $\delta v$  (eq. [6]):

$$\Delta T(v \simeq 0) \simeq T(v \simeq 0) \sqrt{\frac{\Delta v}{N \Delta v_c}} < T_{rms} , \quad (8)$$

where  $T(v \simeq 0)$  is the peak observed antenna temperature. Thus,

$$N > N_{lim} = (S/N)^2 (\Delta v / \Delta v_c) , \quad (9)$$

where the signal-to-noise ratio is defined as the ratio of peak line intensity to the rms fluctuations in the baseline.

These equations suggest that bright, wide lines are the best probes to constrain  $N$  and  $f_0$ . The  $^{12}\text{CO}$  line, which has these properties, will also be optically thick in relatively smaller clumps, which conforms better to our model. If the clumps are optically thick, but shadow each other in phase space, then the above limit (eq. [9]) must be increased by a factor equivalent to the ratio of shadowed (i.e., unseen) clumps to contributing clumps. In this case the above estimate ( $N_{lim}$ ) still provides a good lower limit. However, if there are also cloud-scale gradients in the clump temperatures, the resulting line profile will appear irregularly self-reversed; if interpreted in terms of the simple model under discussion here, one will spuriously underestimate the clump number.

If the clumps emit lines whose widths are larger than thermal, the contribution of one clump will cover more than one spectral channel. In this case the right-hand side of equation (8) has to be corrected downward resulting in a less stringent limit on the number of clumps in the beam

$$N_{cs} > (S/N)^2 \frac{\sqrt{\Delta v^2 + \Delta v_c^2}}{\Delta v_c} . \quad (10)$$

Note that if  $\Delta v_c \simeq \Delta v$ , then the limiting number of clumps in the beam is only determined by the signal-to-noise ratio.

We feel it appropriate to stress again that the simple model sketched in the previous paragraphs will break down if the number of clumps sampled by the beam is small. In this case the use of expectation values is obviously erroneous. Thus, a

very smooth line profile can be either the result of the superposition of a very large number of narrow lines, or of only a few wide profiles with very similar characteristics. These two cases can be distinguished by looking at the positional variations of the line profiles.

In the Kwan & Sanders (1986) model, molecular clouds are made up of small clumps which emit lines of thermal width. The clumps are themselves grouped into larger dynamical structures. The latter (called coherent structures) emit lines whose width is larger than the thermal dispersion, but which are still smaller than the other overall line width. In such a hierarchical molecular cloud, we would then expect to see lumpiness in the emission profiles at two characteristic velocity correlation lengths, one corresponding to individual clump emission widths (typically  $0.2 \text{ km s}^{-1}$  in Orion), and one corresponding to the line width emerging from a coherent structure (assumed by Kwan & Sanders to have a typical value of  $\sim 1 \text{ km s}^{-1}$ ).

The results of the previous section indicate that the amplitude fluctuations for correlation lengths on the order of the thermal widths are below the noise level that we have obtained. If we assume that the individual clumps are in virial equilibrium between their gravitational and thermal energies, that they are spherical with uniform  $\text{H}_2$  density, and if we take  $N_{\text{lim}}$  as the number of clumps sampled by the beam, we can derive expressions for the number, size, and densities of clumps:

$$N_{\text{lim}} \simeq 2.6 \times 10^6 \left( \frac{S/N}{360} \right)^2 \left( \frac{\Delta v}{4 \text{ km s}^{-1}} \right) \left( \frac{0.2 \text{ km s}^{-1}}{\Delta v_c} \right); \quad (11)$$

$$n_c(\text{H}_2) \simeq 8.0 \times 10^{11} \text{ cm}^{-3} \left( \frac{S/N}{360} \right)^4 \left( \frac{\Delta v}{4 \text{ km s}^{-1}} \right)^2 \times \left( \frac{\Delta v_c}{0.2 \text{ km s}^{-1}} \right)^4 \left( \frac{100 M_\odot}{M_{\text{beam}}} \right)^2; \quad (12)$$

$$R_c \simeq 1.07 \text{ AU} \left( \frac{360}{S/N} \right)^2 \left( \frac{4 \text{ km s}^{-1}}{\Delta v} \right) \left( \frac{0.2 \text{ km s}^{-1}}{\Delta v_c} \right) \left( \frac{M_{\text{beam}}}{100 M_\odot} \right). \quad (13)$$

In these expressions  $M_{\text{beam}}$  is the total mass sampled by the beam and is expected to be on the order of  $100 M_\odot$  for a  $45''$  beam size in the region near KL (see Tauber 1990). Clearly, if the line width of a clump is of order the thermal width, the  $\text{H}_2$  densities necessary for virialization (eq. [12]) are unreasonably high. We conclude this on the basis of observations of high-dipole moment molecules (Genzel & Stutzki 1990), which indicate that the highest densities present in this region are of order  $10^7 \text{ cm}^{-3}$  (we note that since most densities derived from high-dipole molecules rely mostly on the analysis of line ratios, they are likely to be largely unaffected by the presence of clumpiness). As a consequence, if there is a set of clumps with individual line widths near the thermal width, they are either bound by a mechanism other than self-gravity or they are transient, short-lived structures.

The volume filling factor of the gas in the cloud can be calculated as the ratio of the smoothed gas density (i.e., the clump gas density averaged over the volume sampled by the antenna beam) to the clump internal gas density. If one assumes that the volume of the cloud covered by the beam is  $\sim \pi \times (0.05 \text{ pc})^2 \times (15 \text{ pc})$ , and the mass in this volume is  $M_{\text{beam}} \simeq 100 M_\odot$ , then the smoothed gas density is on the

order of  $10^5 \text{ cm}^{-3}$ . If the gas densities within clumps are of order  $10^6$ – $10^7 \text{ cm}^{-3}$ , then the volume filling factor of the clumps in the cloud must be less than  $\sim 0.1$ . Thus, if we take  $10^6$  as a lower limit to the number of clumps within the beam (eq. [11]), then the radius of a typical clump must be lower than  $\sim 300 \text{ A.U.}$  The clump mean free path ( $\lambda = 1/n\sigma$ , where  $n$  is the number density of clumps and  $\sigma$  their cross section) and the mean time between collisions ( $\tau = \lambda/v$ , where  $v$  is a typical clump velocity) can now be calculated. For  $10^6$  clumps and  $v \simeq 2 \text{ km s}^{-1}$  these numbers are  $\lambda \simeq 0.02 \text{ pc}$  and  $\tau \simeq 10^4 \text{ yr}$ . Since the mass of a clump in this model is very low ( $10^{-4} M_\odot$ ), a large ( $\sim 10^4$ ) number of collisions will be needed to build up enough mass to form a typical low-mass star, requiring a correspondingly long time of order  $\sim 10^8 \text{ yr}$  if all the clumps are identical. This time scale is much longer than is allowed by the observed age of the Orion cloud ( $\sim 10^7 \text{ yr}$ ) and the number of stars found in its interior (Genzel & Stutzki 1989), even after making allowance for the fact that this crude calculation does not take into account the possibility of gradual growth of clump mass and cross section.

It is possible that individual clumps themselves emit with line widths of order  $1 \text{ km s}^{-1}$ ; this is feasible if a micro-turbulent velocity field exists within each clump. The observations suggest that the fluctuations for velocity correlation lengths of order  $2$ – $3 \text{ km s}^{-1}$  are on the order of a few times the rms in the baseline. If we assume  $\Delta v = 4 \text{ km s}^{-1}$  and  $\Delta v_c = 2 \text{ km s}^{-1}$ , the number of coherent structures predicted by equation (10) to produce the observed smoothness is

$$N_{\text{lim(c.s.)}} \simeq 3.2 \times 10^4 \left( \frac{S/N}{120} \right)^2. \quad (14)$$

Substituting a representative value of the signal-to-noise ratio of 120, and assuming that our beam samples a total mass of  $\sim 100 M_\odot$ , the mass of each clump is then of order  $0.005 M_\odot$ . In this case, if we take  $\sim 10^4$  clumps with velocities of  $\sim 2 \text{ km s}^{-1}$ , the mean free path and mean time between collisions are  $\sim 0.1 \text{ pc}$  and  $\sim 4 \times 10^4 \text{ yr}$ , respectively. Since clumps in this case are more massive than in the thermal width case, the time needed to make a star-forming clump is much shorter, of order  $5 \times 10^6 \text{ yr}$ . While this number is still uncomfortably long compared to the age of the cloud and its rate of star formation, it is more reasonable than that deduced from the thermal clump model.

We can approach the problem of clump properties from the opposite direction by hypothesizing that the narrow features that we see on the profiles arise from individual clumps. Let us assume that the kinetic temperature in the clumps is well represented by the rotation temperature of  $\text{NH}_3$ , which is of order  $30 \text{ K}$  at the 3 N position (Harris et al. 1983). Since the typical antenna temperature of an observed  $^{12}\text{CO}$  feature is  $0.4 \text{ K}$ , its typical brightness temperature will be approximately

$$T_{\text{clump}} \simeq T_{\text{rot}}^*(\text{clump})/(\eta f_0) \simeq 0.8 \text{ K}/f_0, \quad (15)$$

where  $\eta$  is the efficiency of the  $14 \text{ m}$  telescope ( $\sim 0.5$ ), and  $f_0$  is the ratio of the area of a clump to the area of the beam (defined in eq. [6]). If the clump is optically thick, then its brightness temperature will be the kinetic temperature ( $\sim 30 \text{ K}$ ). This implies that the area filling factor of a single clump is  $f_0 \simeq 0.033$ , which corresponds to a volume filling factor of  $\sim 0.006$  and to a clump radius of  $\sim 0.018 \text{ pc}$ . The virial mass of a clump with this radius and with a velocity dispersion of  $\sim 0.7 \text{ km s}^{-1}$  is  $\sim 1 M_\odot$ , and its density is  $\sim 10^6 \text{ cm}^{-3}$ . The latter result is

quite consistent with densities typical of the KL region; further, a mass such as the one calculated is what would be expected of a clump out of which an average star is forming. If the average clump in this region has a mass of order  $0.005 M_{\odot}$ , as is suggested by equation (14), then the range of clump masses must be very large in order to have at least some clumps with masses close to  $1 M_{\odot}$ .

#### 5. SUMMARY AND CONCLUSIONS

We have obtained  $J = 1 \rightarrow 0$  spectra of  $^{12}\text{CO}$  and  $^{13}\text{CO}$  with very high signal-to-noise ratio and spectral resolution toward several positions of the Orion Giant Molecular Cloud. We have analyzed the smoothness of the observed profiles in terms of a simplified model which consists of a clumpy molecular cloud with constant gas volume filling factor and identical clump properties. If the gas units (or clumps) in the model emit lines whose widths are due to thermal motions, then the number of clumps sampled by a  $45''$  beam which is required to reproduce the observed line smoothness is greater than  $\sim 10^6$ . This number is very large and would imply that the masses of individual clumps are extremely low ( $\sim 10^{-4} M_{\odot}$ ) even though from excitation considerations their densities must be fairly high. On the other hand, if clumps are mildly turbulent and emit lines whose widths are of order  $1 \text{ km s}^{-1}$ , the required number of clumps is smaller ( $\sim 10^4$ ), and their masses corre-

spondingly higher. For the former case (thermal clumps) these estimates are limits set by nondetection of fluctuations at the corresponding velocity correlation lengths. On the other hand, there is some evidence in the observed spectra that there are fluctuations in the line profiles at velocity scales corresponding to the case of mildly turbulent clumps.

The small volume filling factors implied by the number of clumps derived and their assumed internal gas density pose problems for the production of stars in the cloud, since coalescence of clumps would occur only over very long time scales. On these grounds the model with mildly turbulent clumps is preferable to that with thermal clumps, but is still only marginally consistent with the observed age of the cloud and its rate of star formation. These considerations move us to propose that the volume filling factor in a significant portion of the cloud must be considerably enhanced over its average value, in order to allow star formation to proceed at a greater rate. In this respect, it seems reasonable to suggest that the volume filling factor near the core of the cloud is enhanced with respect to that near its surface. Finally, we stress that any model which presupposes that clumps are identical can only be a crude approximation. Given that many of the clumps may be transient structures which originate in the turbulent gas flow of their parent cloud, a continuum of sizes and masses is only to be expected.

#### REFERENCES

- Baker, P. L. 1976, *A&A*, 50, 327  
 Bally, J., Langer, W. D., Stark, A. A., & Wilson, R. W. 1987, *ApJ*, 312, L45  
 Bracewell, R. N. 1978, *The Fourier Transform and Its Applications* (New York: McGraw Hill)  
 Genzel, R., & Stutzki, J. 1989, *ARAA*, 27, 41  
 Harris, A., Townes, C. H., Matsakis, D. N., & Palmer, P. 1983, *ApJ*, 290, 359  
 Henry, J. 1979, *Rev. Sci. Instr.*, 50, 185  
 Kutner, M. L., Ulich, B. L. 1981, *ApJ*, 250, 341  
 Kwan, J., & Sanders, D. B. 1986, *ApJ*, 309, 783  
 Mundy, L. G., Cornwell, T. J., Masson, C. R., Scoville, N. Z., Bååth, L. B., & Johansson, L. E. B. 1988, *ApJ*, 325, 382  
 Penzias, A. A., & Burrus, C. A. 1973, *ARAA*, 11, 51  
 Snell, R. L., Mundy, L. G., Goldsmith, P. F., Evans, N. J. II, & Erickson, N. R. 1984, *ApJ*, 276, 625  
 Stutzki, J., & Güsten, R. 1990, *ApJ*, 356, 513  
 Tauber, J. A. 1990, Ph.D. thesis, Univ. of Massachusetts, Amherst  
 Tauber, J. A., & Goldsmith, P. F. 1990, *ApJL*, in press  
 Wilson, T. L., & Johnston, K. J. 1989, *ApJ*, 340, 894